Title
Evidence for breathing modes in direct current, pulsed, and high power impulse magnetron sputtering plasmas

Journal
Applied Physics Letters, 108(3)

ISSN
0003-6951

Authors
Yang, Yuchen
Zhou, Xue
Liu, Jason X
et al.

Publication Date
2016-01-18

DOI
10.1063/1.4939922

Peer reviewed

This manuscript was published on 19 January 2016

Appl. Phys. Lett. 108 (2016) 034101

http://dx.doi.org/10.1063/1.4939922

Evidence for breathing modes in direct current, pulsed, and high power impulse magnetron sputtering plasmas

Yuchen Yang,[1,2] Xue Zhou,[2,3] Jason X. Liu,[2,4] André Anders[2,*]

[1] School of Materials Science and Engineering, State Key Lab for Materials Processing and Die & Mold Technology, Huazhong University of Science and Technology, Wuhan 430074, China
[2] Lawrence Berkeley National Laboratory, 1 Cyclotron Road, Berkeley, California 94720, USA
[3] Department of Electrical Engineering, Harbin Institute of Technology, Harbin 150000, China
[4] Department of Physics, University of California Berkeley, Berkeley, California 94720, USA
* Corresponding author, email: aanders@lbl.gov

We present evidence for breathing modes in magnetron sputtering plasmas: periodic axial variations of plasma parameters with characteristic frequencies between 10-100 kHz. A set of azimuthally distributed probes shows synchronous oscillations of the floating potential. They appear most clearly when considering the intermediate current regime in which the direction of azimuthal spoke motion changes. Breathing oscillations were found to be superimposed on azimuthal spoke motion. Depending on pressure and current, one can also find a regime of chaotic fluctuations and one of stable discharges, the latter at high current. A pressure-current phase diagram for the different situations is proposed.

Low frequency oscillations are ubiquitously observed in all types of $\mathbf{E}\times\mathbf{B}$ discharges and especially well investigated for Hall thrusters.[1] They include low frequency azimuthal modes with moving regions of enhanced ionization, often called spokes. In many cases, a definite number of spokes exists and an azimuthal mode number, $m \geqslant 1$, can be assigned. Rotating spoke oscillations[2-4] have been associated with anomalous (greater than predicted by Bohm) electron cross-field transport.[5] In addition to spokes, Hall thrusters exhibit low frequency bulk oscillations of plasma density and potential known as breathing oscillations.[6] They are correlated with current oscillations and have been extensively studied both experimentally[7] and theoretically.[8]

Similarly to Hall thrusters, sputtering magnetrons also employ an $\mathbf{E}\times\mathbf{B}$ field. Thornton, a pioneer of sputtering magnetrons, anticipated that a whole range of instabilities should occur driven by $\mathbf{E}\times\mathbf{B}$ and density gradients leading to cross-field transport of electrons.[9] Sheridan and Goree[10] followed up on Thornton's suggestions and investigated the scaling of the electron confinement time on the mean-square electric field fluctuations. Using one Langmuir probe, they recorded fluctuations which did not comply with the dispersion relation predicted by turbulence theory, and therefore they concluded that "the observed turbulence is probably not responsible for electron transport." Using a single probe at a distance 5-20 cm from the target, Gudmundsson and coworkers[11] performed a full Langmuir probe analysis for pulsed magnetron discharges and constructed probe *I-V* curves for each time interval, from which electron energy distribution functions and energy density could be derived. This analysis required data integrated over many pulses, in contrast to the time-resolved, multi-probe approach described in this work. None of the above investigations explicitly reported on breathing modes for magnetrons.

Rotating spokes have been thoroughly investigated in recent years for sputtering magnetrons.[12-16] We stress that spoke motion does not imply motion of plasma but rather a displacement of a region of enhanced ionization rate. The spoke velocity is therefore a phase velocity, and not a group velocity. Spoke intensities and shapes have been reported to vary significantly under some conditions.[17] Spokes are the origin of plasma jets and flares[17] which leave the target region, suggesting that electron confinement is disrupted by the spoke's local electric field. The jet or flare velocity was measured for high power impulse magnetron sputtering (HiPIMS) conditions to be about 20,000 m/s, i.e., 3 to 4 times faster than the spoke velocity,[12] indicative that electrons play a critical role for jets and flares.

Over the last few years we have tried to measure local spoke velocity variations not just optically but with sets of neighboring Langmuir probes to gain a deeper understanding of the plasma dynamics and to find conditions for spoke motion reversal.[18] For many conditions, the probe results were surprisingly incomprehensible, with spoke velocities often being indefinite within the measuring accuracy because large potential variations often appeared practically simultaneously at all or most probes. In this work we report on those findings and propose a solution for these puzzling results, namely the simultaneous presence of azimuthal "spoke" and axial "breathing" instabilities, where the latter are similar but not necessarily the same as those observed with Hall thrusters.

While many experiments have been done with pairs of neighboring probes, we focus here on results obtained by using 8 floating probes in combination with an intensified charge-coupled device (ICCD) gated camera, allowing us to simultaneously study the distributions of potential and light emission (which is assumed to be correlated to the ionization rate).

An unbalanced planar magnetron (MeiVac Inc.) with a 76 mm diameter target was used in argon. The magnetic field distribution was published in Fig. 2 of ref.[12]. The gas inlet was more than 45 cm away from the target in the 1 m diameter chamber having a base pressure 1×10^{-4} Pa. Various target materials were studied including 3 mm thick Cr, Cu, Nb, and 6 mm thick Ti and Al. The grounded, annular cylindrical anode was mounted flush with the target.

The eight floating probes, evenly spaced in the azimuthal direction, were positioned 30 mm away above the target surface. Each probe consists of a wire of 0.65 mm diameter and 2 mm length, sticking out of Kapton insulator and pointing towards the magnetron's axis of symmetry. The end point of each probe was positioned right above the racetrack as indicated in Fig. 1.

When investigating direct current magnetron sputtering (DCMS) discharges, a Pinnacle® power supply (Advanced Energy) was used. To eliminate effects that might be caused by voltage fluctuations inherent to the power supply, the supply's output was connected to an RC low-bandpass filter comprised of a 3 kV, 100 μF capacitor and a low inductance resistor (50 Ω to 10 kΩ for currents from 1 A to 10 mA).

When studying pulsed and HiPIMS discharges, a high current pulse generator (SIPP2000 by Melec GmbH) was used. Pulses were 200-1000 μs long with repetition rates between 10 Hz and 40 kHz. The discharge current was measured using a current transformer (Pearson model 101), and the discharge voltage and probes' floating potentials were measured with voltage divider probes (Tektronix P5100). In all plots, the time zero mark indicates the trigger time for the gated camera. All electrical signals were recorded with a National Instruments PXI-5105 oscilloscope. ICCD images of 50 ns exposure time were taken with a Princeton Instruments PIMAX 4 camera, equipped with an f =80 mm Nikon lens. The spectral response of the camera sensor is from 200 to 900 nm. All images are presented using false color "royal" of the image processing software IMAGEJ.[19] Here we focus on results with a chromium target, but similar findings are present with other targets. Floating potentials of all eight probes were systematically recorded for pressures between 0.13 and 2.67 Pa and currents between 0.01 and 300 A.

At a current of 6 A in pulsed MS we are in a regime in which spoke velocity reduction and direction reversal has been found,[18] indicating that at least two different mechanisms lead to a displacement of the region of highest excitation and ionization. This current region was an interesting starting point for the investigations as we anticipated finding and measuring the direction reversal. However, as shown in Fig. 1, we found more-or-less *synchronous* potential variations at all or most probes, which do not indicate spoke motion but suggest a breathing mode. The probes' floating potential oscillations are correlated with oscillations of the discharge current, where the most negative floating potentials correspond to peaks in the current. Through analysis of many fast camera images we noted that images taken at the peaks of current are

brightest, and conversely, images at lowest currents are less intense. This should be expected because current peaks (at constant target voltage) imply peaks of power input to the plasma.

For certain pressure and current conditions, the breathing oscillations appear regular. For example, Figs. 1 (a) and (b) show the oscillations with a characteristic period of approximately 80 μs and 30 μs, while Fig. 1(c) illustrates irregular, faster oscillations (fluctuations) for which one could define an approximate average "period" of 15 μs based on a maximum in a Fast Fourier Transformation. In Figs. 1 (a)-(c), the oscillation amplitudes (δV_{fl}) are approximately 9, 6 and 2.5 V, and the corresponding mean floating potentials (V_{fl}) are approximately -12, -12 and -9 V, yielding $\frac{\delta V_{fl}}{V_{fl}}$ ratios of roughly 75%, 50% and 28%, respectively.

The breathing mode has also been observed with moving spokes when investigating discharges at different currents, suggesting a superposition of spoke and breathing modes. One example is shown in Fig. 2 for DCMS at 4.0 Pa and 40 mA. The images in Figs. 2(b) - (d) were taken at different times, indicating azimuthal spoke motion at low currents.

As recently reported,[20,21] there is a transition from a spoke mode to a spoke-free, azimuthally uniform mode at high current. Indeed, at currents greater than about 190 A, floating potential oscillations disappear and the plasma smoothens out azimuthally. Fig. 3 shows the transition observed at 200 A and 2.67 Pa in HiPIMS. At currents lower than about 190 A, there are azimuthally moving spokes identified by time-delayed phase shifts in the floating potential of neighboring probes. The spoke velocity was determined to be about 8×10^3 m/s, consistent with Ref. 12.

An interesting observation in Fig. 3 is that the current shows a decrease of approximately 10 A coinciding with the onset of instabilities in the probes' signals, implying *increased* plasma impedance, which is unexpected since plasma instabilities disrupt the electrons' confinement.

To further investigate breathing oscillations, four floating probes were placed aligned in the *axial* direction. One was 3 cm from the target, and the others spaced 1 cm further away, with each probe's tips positioned above the racetrack (Fig. 4, right). The result for DCMS at 1 A is shown in Fig. 4: a phase shift of floating potentials is observed. The corresponding velocity is of the order of 1×10^4 m/s, the same order of magnitude found for jets and flares previously observed in HiPIMS.[17] This velocity is faster than the ion thermal $\left(kT_i/m_i\right)^{1/2}$ and ion sound $\left(kT_e/m_i\right)^{1/2}$ velocities, and therefore it can only be related to either ion acceleration in a (traveling) electric field, or due to electrons. With increasing distance from the target, probe signals show splits of peaks and valleys suggesting a complicated picture that is not just a periodic wave or oscillation.

An attempt is made to summarize the observations in a phase map of floating potential characteristics (Fig. 5). At all pressures, the breathing mode is found for currents lower than about 20 A. In the breathing mode, spokes were found to be in motion for DCMS currents lower than 2 A and at pressures higher than approximately 4.0 Pa, whereas they are almost stationary at currents higher than 2 A in pulsed MS or pressures lower than 4.0 Pa in DCMS. Chaotic

behavior is found in HiPIMS at currents between about 20 A and 150 A: the floating potentials of probes are neither periodic nor correlated with each another. Clear azimuthal spoke propagation is found in HiPIMS at currents between about 150 A and 190 A, characterized by regular, sequential floating potential oscillations of all probes, with inconspicuous breathing. A stable mode (spoke-free, no breathing) is found in HiPIMS at currents higher than about 190 A.

The current at the target is a sum of ions arriving and secondary electrons leaving, $I_{disch} = I_i + I_{SE} = I_i\left(1+\gamma_{SE}\right)$. Since the yield of secondary electrons, γ_{SE}, is about 0.1 or even smaller, oscillations of the discharge current can be associated with oscillations of the plasma density. This in turn suggests that the breathing mode is associated with an oscillation of the plasma density, integrated over the target area, i.e., with periodically enhanced ionization. The ionization rate depends on the number densities of atoms to be ionized and of electrons energetic enough to cause ionization. Relatively slow processes (< 100 kHz) are evidence for the strong role of neutral density because charged particles can move on a faster timescale.[8] In contrast to Hall thrusters, the neutral density not only depends on the background gas density but also on the flux of neutrals from the target, including sputtered target atoms and former gas ions.[22] Depending on pressure and current, the contribution of the target flux to the neutral density is different. At very low currents, only small deviations from the background gas density occur. As the current increases, gas rarefaction increases and a feedback loop can be identified: enhanced rarefaction reduces the ionization rate, which reduces the rarefaction, and thus the gas periodically returns. Assuming a characteristic dimension of the gas rarefaction zone of at least 10^{-2} m, and sound speed (less than 10^3 m/s), one arrives at a recovery time of 10^{-5} s or more, or a frequency of 100 kHz or less.

At higher currents, a different “evacuation” mechanism kicks in: a significant ionization of neutrals, followed by removal of ions by the local electric field, i.e., the electric field in the magnetic presheath. This mechanism is predominant for HiPIMS. However, not only is the removal of atoms enhanced but also the supply of atoms consisting of sputtered atoms and gas released from the target by outgassing. The latter is very relevant as those atoms are slow, having essentially the thermal velocity associated with the target temperature, and therefore their density is high.[22] Sputtered atoms are most relevant for target materials of high sputter yield.

The main argument for the breathing mode was the observation of *synchronous* potential variations at azimuthally distributed floating probes. The floating potential is the result of balancing electron and ion currents, $I_{fl.pr.} = I_{pr,i} + I_{pr,e} = 0$. The floating probe adjusts its potential to affect ion and electron currents to its surface. These currents depend on the local plasma density and temperature, or more precisely, on energy distribution functions. Since both plasma density and energy distributions affect the floating potential, floating probe measurements alone are not sufficient to make statements on plasma parameters. The observation of correlated fluctuation of floating potentials, discharge current, and fast imaging allowed us to make statements on oscillating plasma density.

In summary, our experiments revealed that magnetron discharges not only exhibit the well-known azimuthal spoke instability but also a breathing mode instability. The latter is well known

in Hall thrusters and is here suggested to occur for magnetron discharges, although the exact nature of “breathing” remains to be determined. Using sets of floating probes we explored the existence conditions for spoke and breathing modes as a function of current and background gas pressure. We found parameter regions for periodic and chaotic oscillations as well as for stable conditions. The work presents evidence for the breathing mode, however, a deeper interpretation will require further plasma diagnostics and modeling.

This work was done at Lawrence Berkeley National Laboratory with support by the U.S. Department of Energy, under Contract No. DE-AC02-05CH11231. We thank Changchun Sun of the Advanced Light Source for providing the high speed camera. Yuchen Yang and Xue Zhou gratefully acknowledge financial support by the China Scholarship Council.

Fig. 1 Synchronous oscillations of azimuthally placed floating probes. Left: Pulsed magnetron discharge current and potential waveforms for 6 A and (a) 0.13 Pa, (b) 4.0 Pa, (c) 2.7 Pa. Right: Corresponding images were taken at 0 μs.

Fig. 2 Moving spokes observed at 4.0 Pa and 40 mA DC. Image (b) was taken at 0 μs of waveform (a), (c) and (d) were taken at different times.

Fig. 3 Transition from spoke to spoke-free mode in HiPIMS. (a) Discharge current and probe floating potential waveforms, at 2.7 Pa. Images (b) and (c) were taken at -150 μs and 50 μs but for different pulses. Curve 1 (red) has no potential offset, the other curves are shifted for better visibility. The current curve shows a slight impedance increase upon the transition to the spoke mode.

Fig. 4 Floating potentials of four probes aligned in axial direction as indicated on the right; DCMS at 1 A, 0.4 Pa Ar. The black arrows indicate phase shifts associated with a propagation of a wave.

Fig. 5 Floating potential characteristic period contour at Ar pressure from 0.13 Pa to 2.7 Pa and current from 10 mA to 300 A. Modes are indicated as regions separated by white dashed lines.

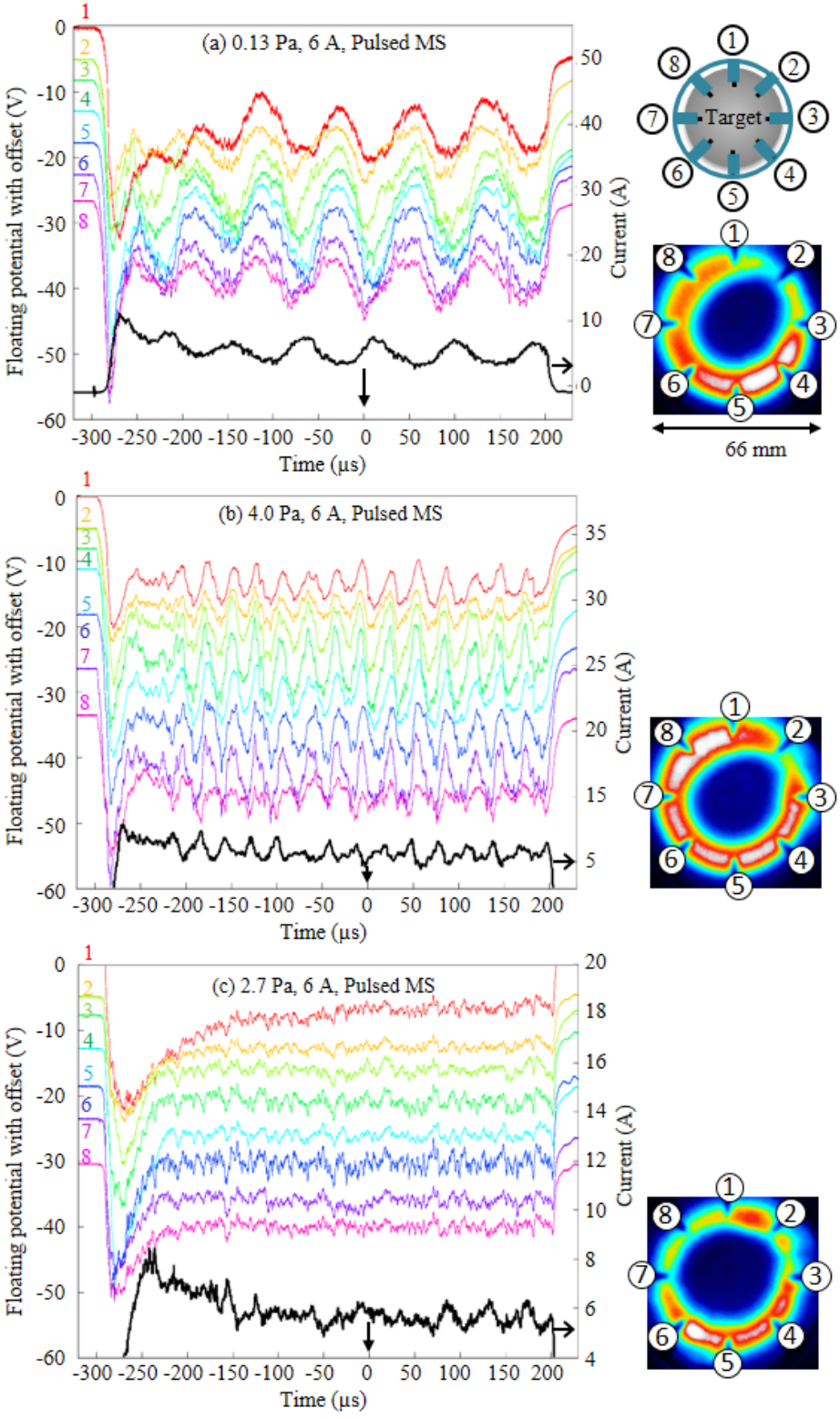
(a) 0.13 Pa, 6 A, Pulsed MS
(b) 4.0 Pa, 6 A, Pulsed MS
(c) 2.7 Pa, 6 A, Pulsed MS
Floating potential with offset (V)
Current (A)
Time (μs)
Target
66 mm

Fig. 1

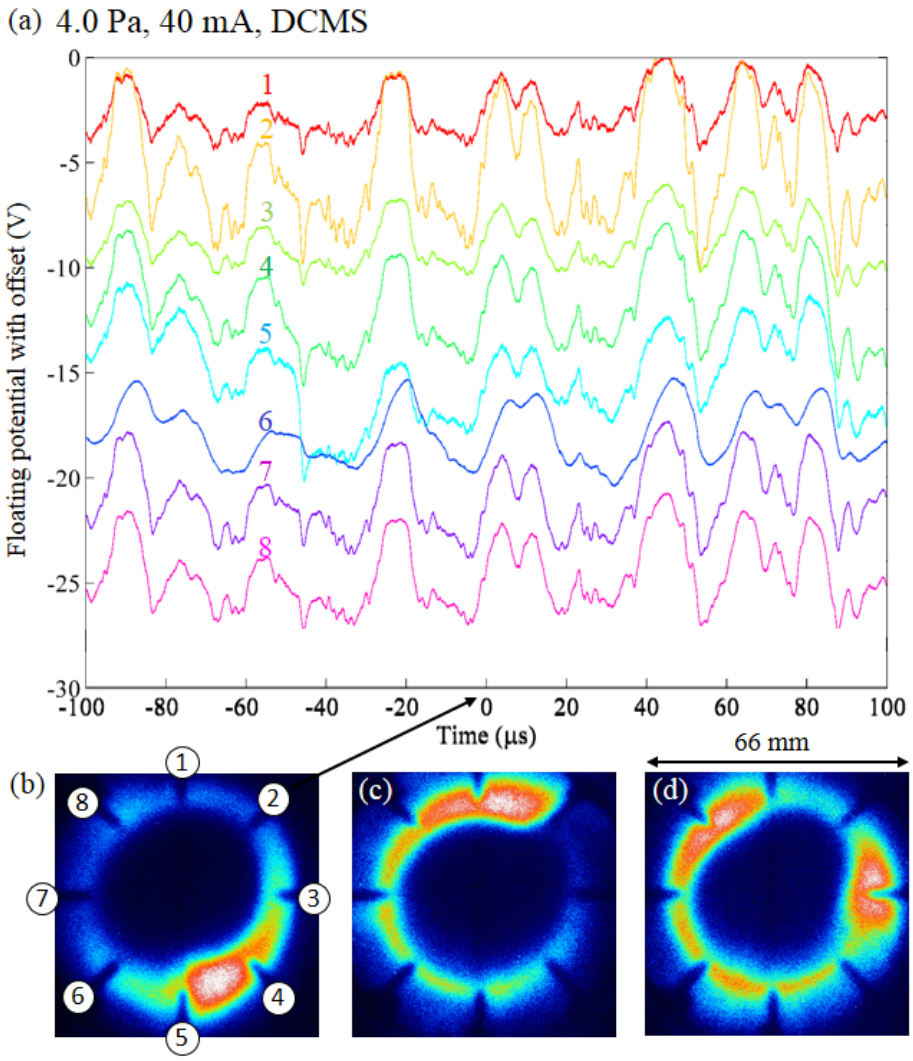
(a) 4.0 Pa, 40 mA, DCMS
Floating potential with offset (V)
0
-5
-10
-15
-20
-25
-30
1
2
3
4
5
6
7
8
-100
-80
-60
-40
-20
0
20
40
60
80
100
Time (μs)
66 mm
(b)
(c)
(d)

Fig. 2

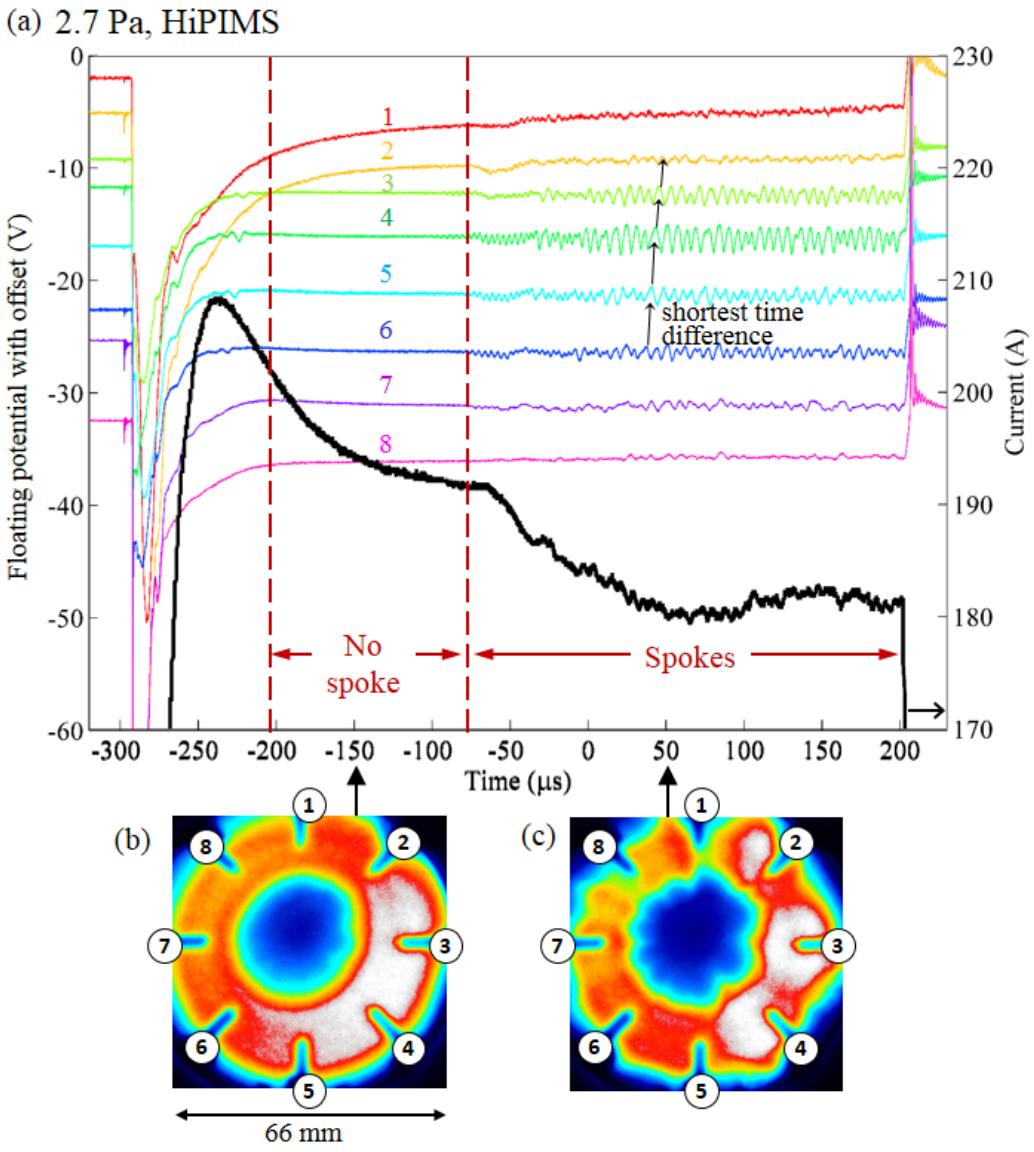
(a) 2.7 Pa, HiPIMS
Floating potential with offset (V)
Current (A)
Time (μs)
shortest time difference
No spoke
Spokes
(b)
(c)
66 mm

Fig. 3

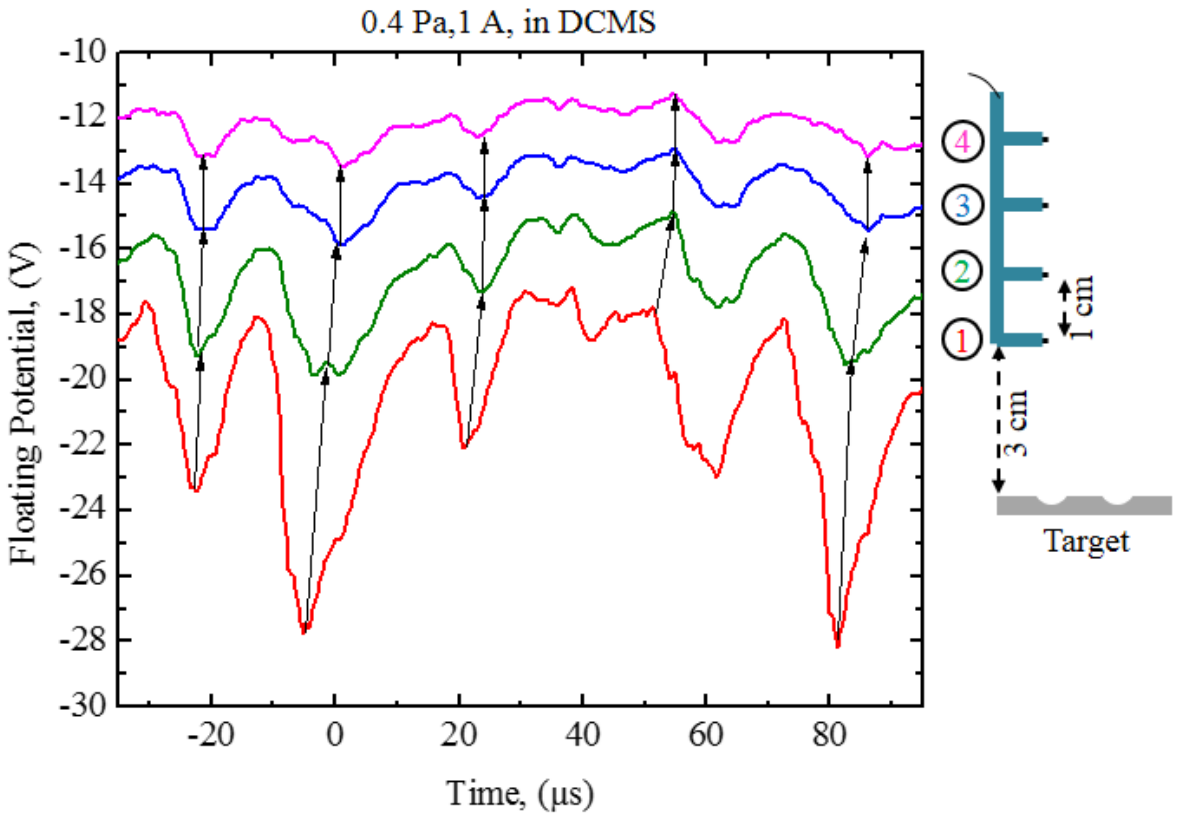
0.4 Pa,1 A, in DCMS
Floating Potential, (V)
-10
-12
-14
-16
-18
-20
-22
-24
-26
-28
-30
-20
0
20
40
60
80
Time, (μs)
4
3
2
1
1 cm
3 cm
Target

Fig. 4

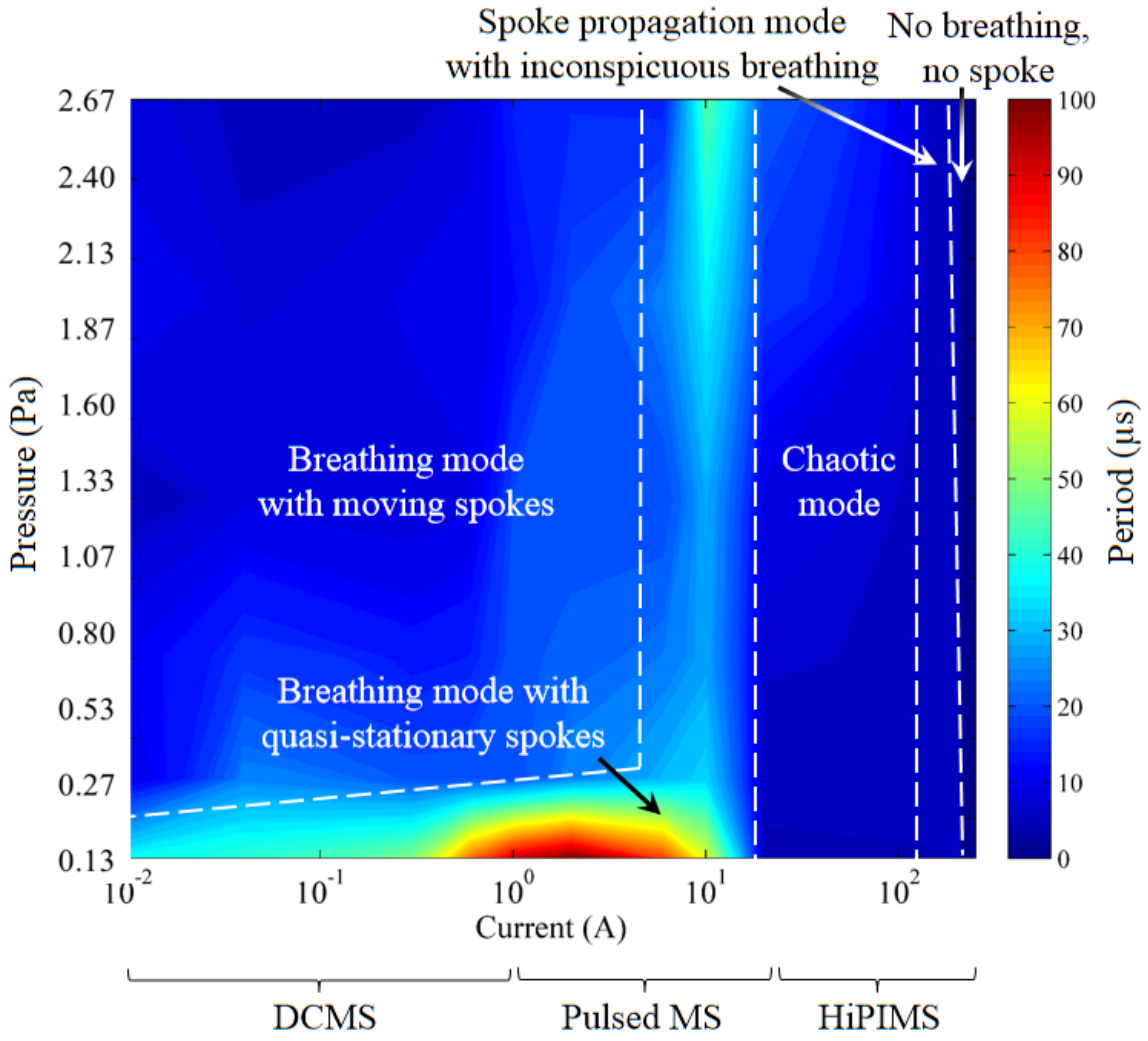
Spoke propagation mode
with inconspicuous breathing
No breathing,
no spoke
Breathing mode
with moving spokes
Chaotic
mode
Breathing mode with
quasi-stationary spokes
Pressure (Pa)
2.67
2.40
2.13
1.87
1.60
1.33
1.07
0.80
0.53
0.27
0.13
Current (A)
Period (µs)
100
90
80
70
60
50
40
30
20
10
0
DCMS
Pulsed MS
HiPIMS

Fig. 5

References

[1] E. Y. Choueiri, Phys. Plasmas **8,** 1411 (2001).
[2] J. B. Parker, Y. Raitses, and N. J. Fisch, Appl. Phys. Lett. **97,** 091501 (2010).
[3] M. J. Sekerak, B. W. Longmier, A. D. Gallimore, D. L. Brown, R. R. Hofer, and J. E. Polk, IEEE Trans. Plasma Sci. **43,** 72 (2015).
[4] D. Escobar and E. Ahedo, IEEE Trans. Plasma Sci. **43,** 149 (2015).
[5] N. Brenning, R. L. Merlino, D. Lundin, M. A. Raadu, and U. Helmersson, Phys. Rev. Lett. **103,** 225003 (2009).
[6] J. P. Boeuf and L. Garrigues, J. Phys. D: Appl. Phys. **84,** 3541 (1998).
[7] C. V. Young, A. Lucca Fabris, and M. A. Cappelli, Appl. Phys. Lett. **106,** 044102 (2015).
[8] S. Barral and E. Ahedo, Physical Review E **79,** 046401 (2009).
[9] J. A. Thornton, J. Vac. Sci. Technol. **15,** 171 (1978).
[10] T. E. Sheridan and J. Goree, J. Vac. Sci. Technol. A **7,** 1014 (1989).
[11] J. T. Gudmundsson, J. Alami, and U. Helmersson, Surf. Coat. Technol. **161,** 249 (2002).
[12] A. Anders, P. Ni, and A. Rauch, J. Appl. Phys. **111,** 053304 (2012).
[13] T. Ito, C. V. Young, and M. A. Cappelli, Appl. Phys. Lett. **106,** 254104 (2015).
[14] A. Hecimovic, M. Böke, and J. Winter, J. Phys. D: Appl. Phys. **47,** 102003 (2014).
[15] A. Kozyrev, N. Sochugov, K. Oskomov, A. Zakharov, and A. Odivanova, Plasma Physics Reports **37,** 621 (2011).
[16] A. Hecimovic, V. Schulz-von der Gathen, M. Böke, A. von Keudell, and J. Winter, Plasma Sources Sci. Technol. **24,** 045005 (2015).
[17] P. A. Ni, C. Hornschuch, M. Panjan, and A. Anders, Appl. Phys. Lett. **101,** 224102 (2012).
[18] Y. Yang, J. Liu, L. Liu, and A. Anders, Appl. Phys. Lett. **105,** 254101 (2014).
[19] W. Rasband, National Institute of Health, 2011, software IMAGEJ 1.44p.
[20] Y. Yang, K. Tanaka, J. Liu, and A. Anders, Appl. Phys. Lett. **106,** 124102 (2015).
[21] T. de los Arcos, V. Layes, Y. Aranda Gonzalvo, V. Schulz-von der Gathen, A. Hecimovic, and J. Winter, J. Phys. D: Appl. Phys. **46,** 335201 (2013).
[22] A. Anders, J. Čapek, M. Hála, and L. Martinu, J. Phys. D: Appl. Phys. **45,** 012003 (2012).